Dendrochronologia 31 (2013) 192–197

Contents lists available at ScienceDirect

Dendrochronologia

journal homepage: www.elsevier.com/locate/dendro

Original article

Development of tree-ring maximum latewood density chronologies for the western Tien Shan Mountains, China: Influence of detrending method and climate response

Yu-jiang Yuan[a], Tong-wen Zhang[a], Wen-shou Wei[a], Daniel Nievergelt[b], Anne Verstege[b], Shu-long Yu[a], Rui-bo Zhang[a], Jan Esper[c,*]

[a] Key Laboratory of Tree-ring Physical and Chemical Research of China Meteorological Administration, Xinjiang Laboratory of Tree Ring Ecology, Institute of Desert Meteorology, China Meteorological Administration, Ürümqi 830002, China
[b] Swiss Federal Research Institute for Forest, Snow and Landscape Research, Birmensdorf 8903, Switzerland
[c] Department of Geography, Johannes Gutenberg University, 55099 Mainz, Germany

ARTICLE INFO

Article history:
Received 24 January 2013
Accepted 30 May 2013

Keywords:
Proxy data
Climate signals
Palaeoclimate
Low frequency trends
Picea schrenkiana

ABSTRACT

Three tree-ring maximum latewood density chronologies were developed from high elevation *Picea schrenkiana* sites in the western Tien Shan Mountains using different detrending methods. The new chronologies extend back to the early 16th and late 17th centuries, and contain significant late spring and summer temperature signals, respectively. An assessment of varying detrending methods and band-pass filtering the chronologies revealed only slightly differing low frequency trends retained in the maximum latewood densities. The distance between sampling sites and the varying seasonality of limiting climatic factors are identified as key drivers affecting the correlation among the maximum latewood density records in the study region. The new chronologies represent reliable proxies of high elevation late spring and summer temperature variability in an area underrepresented by such data, and are ready-to-use for network analyses addressing longer-term climate variations in eastern central Asia.

Introduction

Dendroclimatology is a key method for examining pre-instrumental climate variations. With their precise dating control, annual resolution, and comparability with instrumental meteorological data, tree-ring data have become increasingly valuable in disclosing the long-term dynamics of climate in different regions of the world (Büntgen et al., 2011; Briffa et al., 2001; Cook et al., 2010; Esper et al., 2002, 2007; Liu et al., 2009; Palmer et al., 2006; Shao et al., 2010). New techniques, such as X-ray densitometry, to measure high resolution wood density profiles, have been introduced in dendroclimatic research to assess the association between tree-ring cell formation and climate, and to reconstruct warm season temperature variability at centennial to millennial timescales based on maximum latewood density (MXD) data (Büntgen et al., 2008; Bräuning and Mantwill, 2004; Briffa et al., 1992a; Davi et al., 2003; Esper et al., 2010, 2012a,b; Frank and Esper, 2005; Luckman et al., 1997; Schweingruber et al., 1988; Wang et al., 2002; Wilson and Luckman, 2003).

In recent decades, several dendroclimatological studies based on MXD data have been carried out in China. For example, May–June total precipitation in Huashan in north-central China was reconstructed using ring width and MXD measurements from *Pinus armandii* (Hughes et al., 1994). Wu and Shao (1994) demonstrated that MXD chronologies from the Qinling Mountains contain statistically significant climate variance, and Liu et al. (1997) reconstructed June temperature and April–June precipitation totals over the past 100 years in the Huangling region of the Shanxi Province utilizing minimum earlywood density and stable carbon isotope data. June–September precipitation and April–September temperatures in the Jimusaer region, Xinjiang Province, were reconstructed back to the mid 19th century using tree-ring width and MXD data of spruce trees, and Chen et al. (2009) assessed maximum temperature variations over the growing season based on MXD data from Schrenk Spruce in the Yili region, Xinjiang Province. In the central Hengduan Mountains in southern China, warm season (April–September) temperatures were reconstructed over the past 257 years using MXD data (Fan et al., 2009), and Wang et al. (2010) presented a 306-year climate history for eastern Tibet inferred from MXD. More recently, a 234-year temperature reconstruction was established based on Qinghai spruce MXD data from the central Hexi Corridor, China (Chen et al., 2012).

* Corresponding author. Tel.: +49 6131 3922296.
E-mail address: esper@uni-mainz.de (J. Esper).

1125-7865/$ – see front matter © 2013 Elsevier GmbH. All rights reserved.
http://dx.doi.org/10.1016/j.dendro.2013.05.004

However, an assessment of the impact of detrending methodology and the coherence among regional MXD chronologies from high elevation environments in China, with respect to different frequency domains, is lacking. Furthermore, a thorough understanding of the climatic response characteristics of spruce MXD data from the upper tree-line in the western Tien Shan is still limited.

In this paper, we make use of MXD data from three *Picea schrenkiana* high-elevation sampling sites located the southern Tien Shan Mountains. The data were developed during a scholarly visit in 2007 at Swiss Federal Research Institute WSL. We provide detail on the basic statistics of these newly developed MXD records with respect to differing detrending techniques, and assess the coherence and climate signals of derived mean chronologies. The data will be made available to the International Tree-Ring Databank to set a basis for network analyses of pre-instrumental climate patterns in China and Eastern Central Asia.

Material and methods

Study area and sample collection

Three *P. schrenkiana* tree-line sites were sampled in 2004 and 2006 in the Tien Shan system in northwestern China. These include the sites Jipuke (JPK) in the Boluokenu range, Awuliyaqiaokeshan (AWL) in the Wusun range, and Xiaobaidai (XBD) in the southern Tien Shan Mountains (Fig. 1). In accordance with recordings from the Xinjiang hydrological department, annual precipitation totals are estimated to equal 440 mm, 500 mm, and 710 mm, respectively (Yuan and Li, 1995).

To minimize non-climatic effects on tree growth and latewood development, *P. schrenkiana* trees with no evidence of fire or human disturbance were selected for core sampling in breast height. Two cores (using 5.15 mm diameter increment borers) were extracted from the older trees to support crossdating; only single cores were collected from younger trees. In total, 62 cores from 34 trees were collected in the JPK site, 31 cores from 16 trees in AWL, and 38 cores from 20 trees in XBD. Maximum tree ages range from 480 years in XBD to 780 years in JPK (Table 1).

Tree-ring density measurements and chronology development

Sample preparation followed standard procedures for high-resolution X-ray densitometry measurements (Lenz et al., 1976; Schweingruber et al., 1988). Resin in the tree-ring cores was extracted with 95% alcohol for 48 h. The cores were then cut transversely into laths of 1.00 ± 0.02 mm thickness using a Dendrocut2003 twin-bladed saw, with the angles oriented vertically to the wood fibers adjusted using a dendroscope. The thin-cut wood sections were kept under constant temperature and humidity for 24 h prior to recording the X-ray images. X-ray gray-scale variations were then quantified at ~12 μm resolution using the Walesch Dendro2003 setup, and seven tree-ring parameters (ring width, earlywood width, latewood width, mean earlywood density, mean latewood density, minimum earlywood density, maximum latewood density) derived for each annual ring of the sample collection.

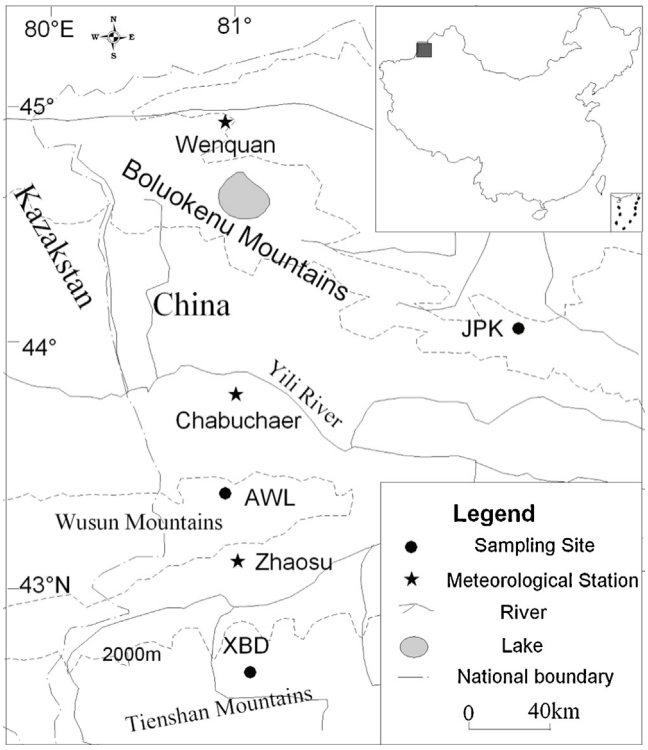

Fig. 1. Location of the *Picea schrenkiana* tree-ring sampling sites and meteorological stations in the western Tien Shan Mountains.

The earlywood–latewood boundaries were identified considering the midpoint between maximum latewood and minimum earlywood densities for each ring. We processed the commonly used MXD parameter in this study.

MXD crossdating was checked using the COFECHA software (Grissino-Mayer, 2001; Holmes, 1983) and verified through comparison with the ring width data. In addition to the statistically based crossdating procedures, all MXD measurement series were assessed and compared with the X-ray images using the Dendro2003 instruments. Even though this is a time-consuming procedure, visual crossdating is required to derive accurately dated MXD timeseries.

The ARSTAN software (Cook and Kairiukstis, 1990) was used for detrending and chronology development. Three detrending techniques were applied to the MXD data at the site level: negative exponential (NE), 300-yr cubic smoothing spline (CSS), and regional curve standardization (RCS) (Briffa et al., 1992b, 1995; Cook and Peters, 1981; Cook et al., 2000; Esper et al., 2002, 2003a; Naurzbaev et al., 2002). In all detrending methods, we calculated ratios from the fitted growth curves; the regional curve in the RCS approach was smoothed using a 67% spline filter (Cook and Peters, 1981; Esper et al., 2003b). Resulting MXD indices were combined into site chronologies by computing bi-weight robust means (see Table 2 for statistical characteristics of the chronologies).

Table 1
MXD sampling sites.

Site code	Latitude (N)	Longitude (E)	Number of trees/cores	Elevation (m)	Aspect	Slope	Canopy density	Maximum tree age
JPK	44°06′20.1″	82°54′50.6″	34/62	~2555	NW-NNE	36°	0.26	780
AWL	43°24′54.6″	81°04′35.7″	16/31	~2690	N-E-WN	33°	0.12	583
XBD	42°44′43.8″	81°15′11.4″	20/38	~2682	SW-NE	8°	0.26	480

Table 2
Statistical characteristics of the NE, CCS, and RCS detrended MXD chronologies over a common 1800–2000 period.

Metric	JPK			AWL			XBD		
	NE	CSS	RCS	NE	CSS	RCS	NE	CSS	RCS
Interseries correlation (trees)	0.18	0.23	0.17	0.18	0.20	0.17	0.23	0.25	0.23
Interseries correlation (all series)	0.19	0.23	0.17	0.19	0.22	0.18	0.24	0.25	0.23
Mean within-tree correlation	0.40	0.38	0.42	0.40	0.40	0.38	0.41	0.42	0.40
First-order autocorrelation	0.37	0.33	0.52	0.31	0.27	0.33	0.32	0.27	0.31
Signal-to-noise ratio	5.76	7.55	5.27	4.24	4.92	4.07	7.37	8.17	7.21
Variance of first eigenvector (%)	23.2	27.2	22.1	24.4	26.5	23.7	28.0	29.4	28.4
Expressed population signal	0.85	0.88	0.84	0.81	0.83	0.80	0.88	0.89	0.88
First year SSS >0.85 (tree number)	1539 (12)	1526 (10)	1539 (12)	1691 (10)	1691 (9)	1691 (10)	1689 (10)	1688 (9)	1689 (10)

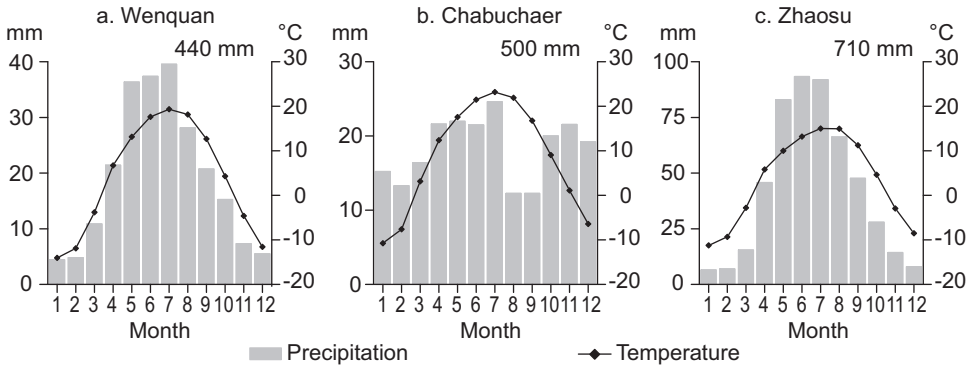

Fig. 2. Climate diagrams of the meteorological stations in (a) Wenquan, (b) Chabuchaer, and (c) Zhaosu in the western Tien Shan Mountains, China. Bars indicate monthly precipitation totals (mm), curves indicate monthly mean temperatures (°C).

Meteorological data

For climate signal detection, monthly temperature means and precipitation totals of three meteorological stations in the vicinity of the sampling sites (JPK, AWL, XBD) were used (obtained from the China Meteorological Data Sharing Service System; http://cdc.cma.gov.cn/). These include the Wenquan station in 1354 m asl (81°01′ E, 44°58′ N) covering the 1959–2004 period, the Chabuchaer station in 601 m asl (81°09′ E, 43°51′ N) covering the 1961–2005 period, and the Zhaosu station in 1855 m asl (81°08′ E, 43°09′ N) covering the 1956–2006. Whereas the seasonal temperature patterns are quite similar among these stations, precipitation totals indicate more pronounced summer peaks in Wenquan and Zhaosu (Fig. 2).

Coherence and climate response analysis

For the assessment of frequency-dependent coherence among the MXD data, the differently detrended site chronologies were decomposed into high-pass and low-pass components using ~8-year reciprocal filters (Fritts, 1976). Pearson correlation coefficients were considered to quantify the significance of detrending methodology and frequency decomposition on MXD chronologies. In order to estimate climate signals inherent to the site chronologies, we calculated Pearson correlation coefficients between the MXD chronologies and monthly temperature and precipitation data from the corresponding meteorological stations over the common periods of overlap.

Results and discussion

Impact of detrending method on MXD chronologies

While the differences among the differently detrended chronologies are mostly statistically insignificant within each site, JPK, AWL, and XBD, the CSS detrending tends to produce slightly higher interseries correlations at the tree and core level, but lower within-tree correlations, compared to the NE and RCS detrendings (Table 2). The first-order autocorrelation is generally higher after RCS detrending (max. 0.52 in the JPK chronology) compared to the

Table 3
Coherence among differently detrended MXD chronologies. Table lists correlation coefficients (r) and numbers of pairs (n) for each sampling site, JPK, AWL, and XBD. NE refers to negative exponential, CSS to 300-yr cubic smoothing spline, and RCS to regional curve standardization methods. Results for the original, high-, and low-pass filtered chronologies are shown.

	JPK			AWL			XBD		
	NE-CSS	NE-RCS	CSS-RCS	NE-CSS	NE-RCS	CSS-RCS	NE-CSS	NE-RCS	CSS-RCS
Original									
r	0.99	0.94	0.97	0.99	0.98	0.98	0.99	0.94	0.96
n	466	466	466	316	316	316	318	318	318
High frequency									
r	1.00	1.00	1.00	0.99	0.98	0.99	1.00	0.99	0.99
n	454	454	454	304	304	304	306	306	306
Low frequency									
r	0.98	0.84	0.90	0.99	0.97	0.97	0.98	0.85	0.93
n	454	454	454	304	304	304	306	306	306

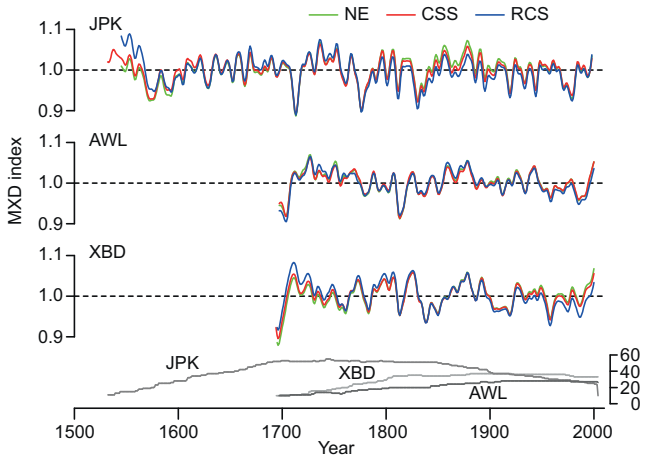

Fig. 3. Comparison of differently detrended MXD site chronologies. Smoothed (~10-year fliter) MXD chronologies of sites JPK, AWL, and XBD after detrending using the NE (green), CSS (red), and RCS (blue) methods over the past 300–500 years. Bottom panel shows the replication (number of measurement series) throughout time. (For interpretation of the references to colour in this figure legend, the reader is referred to the web version of this article.)

NE and CSS detrendings (min. 0.27 in the AWL and XBD chronologies with CSS detrending) pointing to an increased low frequency loading inherent to the chronologies developed using one single growth curve at each site (RCS). As a consequence, the differently detrended site chronologies correlate all ≥0.98 after high-pass filtering, but differ substantially (though still statistically significant; min. correlation = 0.84 for the NE and RCS detrended JPK chronologies) after low-pass filtering – except for the AWL site chronologies that are similar throughout the frequency domains (Table 3).

These larger (JPK and XBD chronologies) and smaller (AWL chronology) differences in the low frequency domain are further emphasized by plotting the smoothed site chronologies (Fig. 3). Whereas the AWL chronologies are rather similar throughout the past three centuries, the RCS chronologies from the JPK and XBD sampling sites contain more low frequency variability compared to their NE and particularly the CSS detrended counterparts. For example, in JPK, the RCS detrended record shows lower chronology levels throughout the 19th and much of the 20th centuries; and in XBD, the RCS chronology indicates lower values after about 1930. The differences are also substantial during the early chronology periods (before 1560 in JPK, and before 1750 in XBD), but these deviations are also affected by reduced sample replications typical to records derived from only living trees.

Inter-site comparison

The coherence among the chronologies from the different sites in the western Tien Shan region is a function of geographic distance and chronology frequency domain. Using the NE detrended site chronologies, we found higher (and more balanced) correlations among the sampling sites in the high frequency domain (ranging from 0.52 to 0.70), and lower correlations in the low frequency domain (from 0.10 to 0.50; Table 4). The generally increased coherence among the high-pass filtered timeseries points to the strength of MXD chronologies in the high frequency domain to retain common inter-annual climate variations in geographically limited regions (e.g., Esper et al., 2010).

Furthermore, the AWL and XBD chronologies share highest correlation coefficients throughout all frequency domains (ranging from 0.50 to 0.70), whereas the JPK and XBD chronologies correlate weakest (from 0.10 to 0.52; Table 4). These differences seem to be

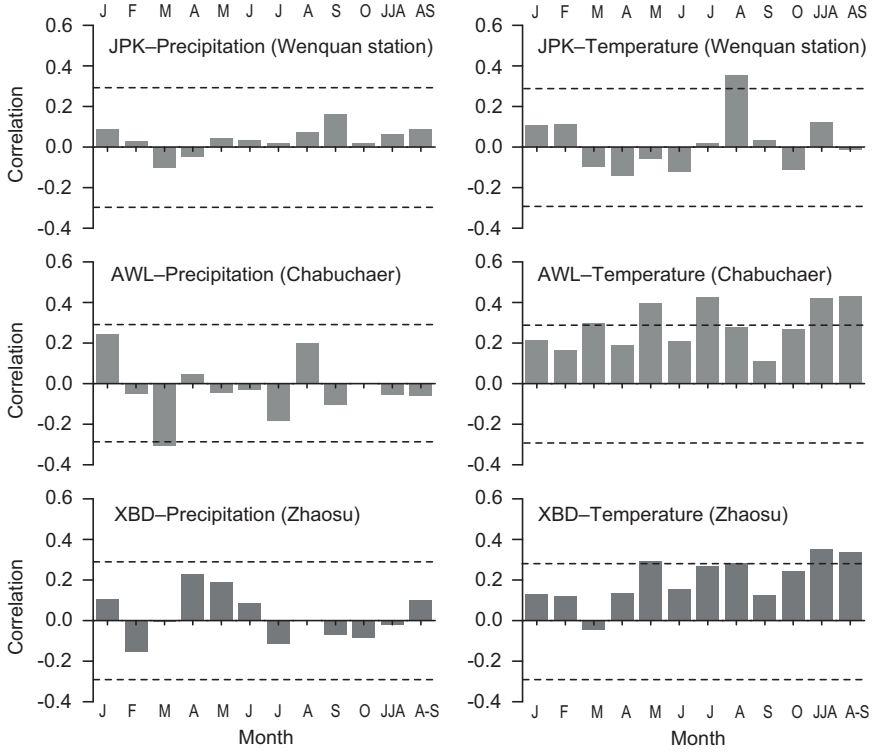

Fig. 4. Correlations between NE detrended site chronologies (JPK, AWL, XBD) and monthly (seasonal) precipitation and temperature data. Nearby meteorological stations are Wenquan for the JPK site (1959–2004 period), Chabuchaer for the AWL site (1961–2005 period), and Zhaosu for the XBD site 1956–2006 period). Dashed lines indicate 95% significance levels, corrected for first-order autocorrelation. On the *x*-axis, JJA refers to the seasonal mean including June, July and August, and A–S to the mean from August to September.

Table 4
Coherence among NE-detrended MXD site chronologies. Table shows correlation coefficients (r), significance values (p), and numbers of pairs (n). Results for the original, high-, and low-pass filtered chronologies are shown.

	JPK-AWL	JPK-XBD	AWL-XBD
Original			
r	0.44	0.36	0.64
p	0.01	0.01	0.01
n	314	314	314
High frequency			
r	0.55	0.52	0.70
p	0.01	0.01	0.01
n	302	302	302
Low frequency			
r	0.26	0.10	0.50
p	0.01	0.07	0.01
n	302	302	302

related to the geographic location and distance between the sampling sites. Both the AWL and XBD sites are located nearby in Yili River Basin where the regional climatic regime appears more uniform, while the JPK and XBD sampling sites are located in greater distance to each other, in the Yili River Basin and northern slope of the Tien Shan Mountains, respectively. Consequently, the medium distance between JPK and AWL sites (compared to the other combinations) results in medium correlations between the respective MXD chronologies, a finding valid for all frequency domains.

Climatic signals

Climate-growth relationships were assessed through simple correlation analysis of the NE detrended MXD chronologies with monthly precipitation and temperature data from nearby meteorological stations (Fig. 4; similar results were obtained using the alternative detrendings). For the JPK sampling site, we used observational data from the Wenquan meteorological station, as past experience based on the analysis of tree-ring width network (Pan et al., 2007a,b; Yang et al., 2006) indicated this station from the Bozhou region to be most representative (Fig. 1). Results indicate prevailing warm season temperature signals inherent to the MXD chronologies, with maximum responses to late spring and late summer months in AWL and XBD, and to August in JPK. All other correlations with precipitation (and temperature) – except for a negative coefficient with March precipitation totals at the AWL site ($r = -0.31$, $p < 0.05$, $n = 45$) – remain insignificant, pointing to the distinct importance of growing season temperatures on spruce density formation in high elevation western Tien Shan sites. These results are consistent with previous studies on the climatic response of MXD chronologies from other areas and based on differing tree species (Büntgen et al., 2006; Chen et al., 2012; Davi et al., 2003; Frank and Esper, 2005; Esper et al., 2010; Wang et al., 2002, 2010). The similarity of summer temperature correlation patterns between the nearby AWL and XBD chronologies (Fig. 4d and f) indicates that these MXD records in the vicinity of the Yili River Basin are affected by similar climatic variations.

Conclusions

Using negative exponential functions, 300-year cubic smoothing splines, and the regional curve standardization method, differently detrended MXD chronologies were developed for three *P. schrenkiana* sites in the western Tien Shan Mountains. An assessment of the resulting timeseries revealed minor differences due to detrending methodology in the high frequency domain, but substantial deviations after low pass filtering the MXD chronologies (in two out of three cases). Coherence among the site chronologies is related to the distance between sampling sites as well as the timeseries frequency domains. Inter-site coherence is larger in the high frequency domain and lower in the low frequency domain, indicating strength of the MXD chronologies in retaining common high frequency variance. Detection of common lower frequency temperature variance might require the development of further MXD (and TRW) data in the region, including chronologies based on relict (plus living) tree measurements that enable additional assessments of detrending choices and potential constrains toward the lower end of the frequency spectrum. All MXD site records contain significant late spring and summer temperature signals, though the month of maximum response varies from May to July and August. The MXD data from the western Tien Shan Mountains presented here, represents a collection of some of the best-replicated, high resolution density chronologies worldwide, and will substantially increase the potential to reconstruct summer temperature variation in Central Asia over the past 300–500 years.

Acknowledgments

Supported by Meteorology Public Welfare Industry (Special Research Projects GYHY201106013 and GYHY201206014), the National Natural Science Foundation of China (NSFC Projects 41275120, 41071072, 40975056, 41205070, 41205124, and 41271098), and the National Basic Research Program of China (Program 973, 2010CB951001).

References

Bräuning, A., Mantwill, B., 2004. Summer temperature and summer monsoon history on the Tibetan Plateau during the last 400 years recorded by tree rings. Geophysical Research Letters 31, L24205, http://dx.doi.org/10.1029/2004GL020793.
Briffa, K.R., Jones, P.D., Schweingruber, F.H., 1992a. Tree-ring density reconstructions of summer temperature patterns across western North America since 1600. Journal of Climate 5, 735–754.
Briffa, K.R., Jones, P.D., Bartholin, T.S., Eckstein, D., Schweingruber, F.H., Karlén, W., Zetterberg, P., Eronen, M., 1992b. Fennoscandian summers from AD 500: Temperature changes on short and long timescales. Climate Dynamics 7, 111–119.
Briffa, K.R., Jones, P.D., Schweingruber, F.H., Shiyatov, S., Cook, E.R., 1995. Unusual twentieth-century summer warmth in a 1,000-year temperature record from Siberia. Nature 376, 156–159.
Briffa, K.R., Osborn, T.J., Schweingruber, F.H., Harris, I.C., Jones, P.D., Shiyatov, S.G., Vaganov, E.A., 2001. Low-frequency temperature variations from a northern tree ring density network. Journal of Geophysical Research 106, 2929–2941.
Büntgen, U., Frank, D.C., Nievergelt, D., Esper, J., 2006. Summer temperature variations in the European Alps, A.D. 755–2004. Journal of Climate 19, 5606–5623.
Büntgen, U., Frank, D., Grudd, H., Esper, J., 2008. Long-term summer temperature variations in the Pyrenees. Climate Dynamics 31, 615–631.
Büntgen, U., Tegel, W., Nicolussi, K., McCormick, M., Frank, D., Trouet, V., Kaplan, J.O., Herzig, F., Heussner, K.U., Wanner, H., Luterbacher, J., Esper, J., 2011. 2500 years of European climate variability and human susceptibility. Science 331, 578–582.
Chen, J., Wang, L.L., Zhu, H.F., Wu, P., 2009. Reconstructing mean maximum temperature of growing season from the maximum density of the Schrenk Spruce in Yili, Xinjiang, China. Chinese Science Bulletin 54, 2300–2308.
Chen, F., Yuan, Y.J., Wei, W.S., Yu, S.L., Fan, Z.A., Zhang, R.B., Zhang, T.W., Qin, L., Shang, H.M., 2012. Temperature reconstruction from tree-ring maximum latewood density of Qinghai spruce in middle Hexi Corridor, China. Theoretical and Applied Climatology 107, 633–643.
Cook, E.R., Peters, K., 1981. The smoothing spline: a new approach to standardizing forest interior tree-ring width series for dendroclimatic studies. Tree-Ring Bulletin 41, 45–53.
Cook, E.R., Kairiukstis, L.A., 1990. Methods of Dendrochronology. Kluwer Academic Publishers, Dordrecht, pp. 408.
Cook, E.R., Buckley, B.M., D'Arrigo, R.D., Peterson, M.J., 2000. Warm-season temperatures since 1600 BC reconstructed from Tasmanian tree rings and their relationship to large-scale sea surface temperature anomalies. Climate Dynamics 16, 79–91.
Cook, E.R., Anchukaitis, K.J., Buckley, B.M., D'Arrigo, R.D., Jacoby, G.C., Wright, W.E., 2010. Asian monsoon failure and mega drought during the last millennium. Science 328, 486–489.
Davi, N.K., Jacoby, G.C., Wiles, G.C., 2003. Boreal temperature variability inferred from maximum latewood density and tree-ring width data, Wrangell Mountain region, Alaska. Quaternary Research 60, 252–262.

Esper, J., Cook, E.R., Schweingruber, F.H., 2002. Low-frequency signals in long tree-ring chronologies for reconstructing past temperature variability. Science 295, 2250–2253.
Esper, J., Cook, E.R., Krusic, P.J., Peters, K., Schweingruber, F.H., 2003a. Tests of the RCS method for preserving low-frequency variability in long tree-ring chronologies. Tree-Ring Research 59, 81–98.
Esper, J., Shiyatov, S.G., Mazepa, V.S., Wilson, R.J.S., Graybill, D.A., Funkhouser, G., 2003b. Temperature-sensitive Tien Shan tree ring chronologies show multi-centennial growth trends. Climate Dynamics 21, 699–706.
Esper, J., Frank, D.C., Büntgen, U., Verstege, A., Luterbacher, J., Xoplaki, E., 2007. Long-term drought severity variations in Morocco. Geophysical Research Letters 34, http://dx.doi.org/10.1029/2007GL030844.
Esper, J., Frank, D.C., Büntgen, U., Verstege, A., Hantemirov, R.M., Kirdyanov, A.V., 2010. Trends and uncertainties in Siberian indicators of 20th century warming. Global Change Biology 16, 386–398.
Esper, J., Büntgen, U., Timonen, M., Frank, D.C., 2012a. Variability and extremes of Northern Scandinavian summer temperatures over the past two millennia. Global and Planetary Change 88–89, 1–9.
Esper, J., Frank, D.C., Timonen, M., Zorita, E., Wilson, R.J.S., Luterbacher, J., Holzkämper, S., Fischer, N., Wagner, S., Nievergelt, D., Verstege, A., Büntgen, U., 2012b. Orbital forcing of tree-ring data. Nature Climate Change 2, 862–866.
Fan, Z.X., Bräuning, A., Yang, B., Cao, K.F., 2009. Tree ring density-based summer temperature reconstruction for the central Hengduan Mountains in southern China. Global and Planetary Change 65, 1–11.
Frank, D., Esper, J., 2005. Characterization and climate response patterns of a high-elevation, multi-species tree-ring network in the European Alps. Dendrochronologia 22, 107–121.
Fritts, H.C., 1976. Tree Rings and Climate. Academic Press, London, pp. 567.
Grissino-Mayer, H.D., 2001. Evaluating crossdating accuracy: a manual and tutorial for the computer program COFECHA. Tree-Ring Research 57, 205–221.
Holmes, R.L., 1983. Computer-assisted quality control in tree-ring data and measurement. Tree-ring Bulletin 43, 69–78.
Hughes, M.K., Wu, X.D., Shao, X.M., Garfin, G.M., 1994. A preliminary reconstruction of rainfall in North-Central China since A.D. 1600 from tree-ring density and width. Quaternary Research 42, 88–99.
Lenz, O., Schaer, E., Schweingruber, F.H., 1976. Methodische Probleme bei der radiographisch-densitometrischen Bestimmung der Dichte und der Jahrringbreiten von Holz. Holzforschung 30, 114–123.
Liu, Y., Wu, X.D., An, Z.S., Zhu, Y.Z., Shao, X.M., Liu, H.B., Li, Z.Y., 1997. Tree-ring density and stable carbon isotope based seasonal precipitation and temperature reconstruction for the Huangling region in Shanxi Province, China. Science in China Series D: Earth Sciences 27, 271–276 (in Chinese, with English abstract).
Liu, Y., An, Z.S., Linderholm, H.W., Chen, D.L., Song, H.M., Cai, Q.F., Sun, J.Y., Tian, H., 2009. Annual temperatures during the last 2485 years in the mid-eastern Tibetan Plateau inferred from tree rings. Science in China Series D: Earth Sciences 52, 348–359.
Luckman, B.H., Briffa, K.R., Jones, P.D., Schweingruber, F.H., 1997. Tree-ring based reconstruction of summer temperatures at the Columbia Icefield, Alberta, Canada, AD 1073–1983. The Holocene 7, 375–389.
Naurzbaev, M.M., Vaganov, E.A., Sidorova, O.V., Schweingruber, F.H., 2002. Summer temperatures in eastern Taimyr inferred from a 2427-year late-Holocene tree-ring chronology and earlier floating series. The Holocene 12, 727–736.
Palmer, J., Lorrey, A., Turney, C.S.M., Hogg, A., Baillie, M., Fifield, K., Ogden, J., 2006. Extension of New Zealand kauri (*Agathis australis*) tree-ring chronologies into Oxygen Isotope Stage (OIS) 3. Journal of Quaternary Science 21, 779–787.
Pan, Y.T., Yuan, Y.J., Yu, S.L., 2007a. Reconstruction and analysis of summer temperature sequence for Boertala River basin over past 461 years. Journal of Desert Research 27, 159–164 (in Chinese, with English abstract).
Pan, Y.T., Yuan, Y.J., Yu, S.L., Jin, H.L., 2007b. Feasible study on the deduced paleoclimate change using image analysis of tree-ring from the Bortala River basin. Arid Zone Research 24, 255–260 (in Chinese, with English abstract).
Schweingruber, F.H., Bartholin, T., Schaur, E., Briffa, K.R., 1988. Radiodensitometric-dendroclimatological conifer chronologies from Lapland (Scandinavia) and the Alps (Switzerland). Boreas 17, 559–566.
Shao, X., Xu, Y., Yin, Z.Y., Liang, E., Zhu, H., Wang, S., 2010. Climatic implications of a 3585-year tree-ring width chronology from the northeastern Qinghai-Tibetan Plateau. Quaternary Science Reviews 29, 2111–2122.
Wang, L., Payette, S., Bégin, Y., 2002. Relationships between anatomical and densitometric characteristics of black spruce and summer temperature at tree line in northern Quebec. Canadian Journal of Forest Research 32, 477–486.
Wang, L., Duan, J.P., Chen, J., Huang, L., Shao, X.M., 2010. Temperature reconstruction from tree-ring maximum density of *Balfour spruce* in eastern Tibet, China. International Journal of Climatology 30, 972–979.
Wilson, R.J.S., Luckman, B.H., 2003. Dendroclimatic reconstruction of maximum summer temperatures from upper tree-line sites in Interior British Columbia, Canada. The Holocene 13, 851–861.
Wu, X.D., Shao, X.M., 1994. A preliminary analysis on response of tree-ring density to climate in the Qinling Mountains of China. Quarterly Journal of Applied Meteorology 5, 253–256 (in Chinese, with English abstract).
Yang, J.H., Jiang, Z.H., Wei, F., Wu, S.A., 2006. Variability of extreme high temperature and low temperature and their response to regional warming in Northwest China in recent 45 years. Arid Land Geography 29, 625–631 (in Chinese, with English abstract).
Yuan, Y.J., Li, J.F., 1995. The response functions of tree-ring chronologies in Western Tianshan Mountains. Journal of Glaciology and Geocryology 17, 170–177 (in Chinese, with English abstract).